Ab initio MRCI+Q study on low-lying states of CS including spin-orbit coupling

ARTICLE *in* THE JOURNAL OF PHYSICAL CHEMISTRY A · MARCH 2013

Impact Factor: 2.69 · DOI: 10.1021/jp4002516 · Source: PubMed

6 AUTHORS, INCLUDING:

Rui Li
Jilin University
14 PUBLICATIONS **32** CITATIONS
SEE PROFILE

Bing Yan
Jilin University
47 PUBLICATIONS **63** CITATIONS
SEE PROFILE

THE JOURNAL OF PHYSICAL CHEMISTRY A

Article

pubs.acs.org/JPCA

Ab Initio MRCI+Q Study on Low-Lying States of CS Including Spin−Orbit Coupling

Rui Li,[†,‡] Changli Wei,[†] Qixiang Sun,[†] Erping Sun,[†] Haifeng Xu,*[,†] and Bing Yan*[,†]

[†]Institute of Atomic and Molecular Physics, Jilin University, Changchun 130012, China

[‡]Department of Physics, College of Science, Qiqihar University, Qiqihar 161006, China

Supporting Information

ABSTRACT: Carbon monosulfide (CS), which plays an important role in a variety of research fields, has long received considerable interest. Due to its transient nature and large state density, the electronic states of CS have not been well understood, especially the interactions between different states. In this paper, we performed a detail ab initio study on the low-lying electronic states of CS by means of the internally contracted multireference configuration interaction method (including Davidson correction) with scalar relativistic correction using the Douglas−Kroll−Hess Hamiltonian. We focused on the spin−orbit coupling of the states via the state interaction method with the full Breit−Pauli Hamiltonian. The potential energy curves (PECs) of 18 Λ−S states correlated with the lowest dissociation limit of the CS molecule were calculated, as well as those of 50 Ω states generated from the Λ−S states. The spectroscopic constants of the bound states were obtained, which are in good agreement with previous available experimental and theoretical results. The state perturbations of the $a^3\Pi$ and $A^1\Pi$ states with other low-lying electronic states are discussed in detail, based on the calculated spin−orbit matrix as well as the PECs of the Ω states. Avoided crossing in the states of CS was indicated when spin−orbit coupling was taken into account. Finally, the allowed transition dipole moments as well as the lifetimes of the five lowest vibrational states of the $A^1\Pi_1$, $A'^1\Sigma^+_{0^+}$ and $a^3\Pi_i$ states were obtained.

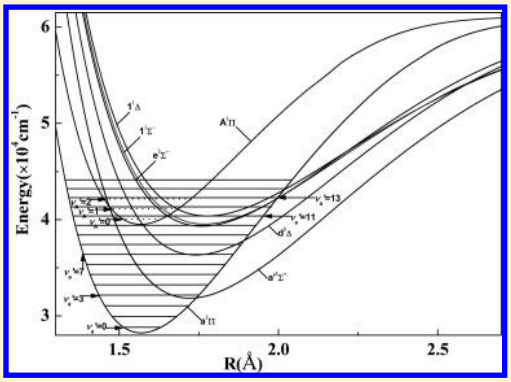

INTRODUCTION

Carbon monosulfide (CS) is an important molecule in astrophysical environments that is abundant in space such as comets,[1] the star-forming region,[2] interstellar clouds,[3] molecular clouds,[4] and other galaxies.[5] CS is viewed to be related to formation of sulfide, which may cause acid rain and lead to stratospheric ozone depletion and global climate change. For example, CS may produce atmospheric carbon sulfide; it is the main dissociation fragment of CS_2, which is one significant reagent to produce sulfides. CS is also believed to be a main constitute of plasmas with sulfur-containing precursors. Due to its importance in a variety of research fields, investigation of the electronic states and the spectrum of CS has been continuously attracting interest over many years.

CS is a short-lived and unstable diatomic molecule; thus, it is usually treated as a radical even though there are no unpaired electrons in its ground state. In addition, CS exhibits a very high density of the electronic states, resulting in complicated couplings among different degrees of freedom, such as avoided crossing, spin−orbit coupling (SOC), and so forth. Regarding the facts of the transient nature as well as the strong interaction of electronic excited states, spectroscopic properties of CS still remain a challenging task to both experimental and theoretical studies.

Since the pioneering work of the $A^1\Pi-X^1\Sigma^+$ emission spectrum of CS was photographed by Crawford et al. in 1934,[6] many spectroscopic studies have been carried out on the low-lying electronic states of CS. The lowest singlet excited state $A^1\Pi$ has been investigated experimentally by quite a few groups during the past several decades. The emission band of $A^1\Pi-X^1\Sigma^+$ was recorded, and the radiative lifetimes of different vibrational states of $A^1\Pi$ were measured.[7−10] The second singlet excited state $A'^1\Sigma^+$ was studied using the time-resolved fluorescence method,[11] which showed much shorter lifetimes than those in the $A^1\Pi$ state. The spin-forbidden transition, $a^3\Pi-X^1\Sigma^+$ of CS was also observed at high resolution in the near-ultraviolet region,[12] and the lifetimes of the $a^3\Pi_0$ and $a^3\Pi_1$ sublevels were determined by time-resolved spectroscopy experiments.[13] Compared with the singlet band, absorption or emission in the triplet manifold, for example $d^3\Delta-a^3\Pi$, is more difficult to analyze because the strong perturbations between $d^3\Delta$ ($a^3\Pi$) and $A^1\Pi$ states cause extra lines and level shifts that greatly complicate the spectrum.[14−16]

Along with experimental studies, several theoretical efforts were also made to investigate the low-lying excited states for CS. Early studies included calculation of eigenvalues, transition dipole moments, and spectroscopic parameters of the low-lying Λ−S states by the SCF-CI method[17] and the ground state of

Received: January 9, 2013
Revised: February 22, 2013
Published: February 22, 2013

CS by means of diagrammatic perturbation theory.[18] In 1998, Ornellas produced accurate potential energy curves (PECs) for the $X^1\Sigma^+$ and $A^1\Pi$ states using the CASSCF/MRCISD approach, in which transition dipole moment functions, Franck−Condon factors, and radiative lifetimes for the $A^1\Pi$ state were also obtained.[19] Due to the exclusion of singlet−triplet perturbations in his calculation, the lifetime of $A^1\Pi$ ($\nu' = 0$) is about 20−95 ns shorter than the reported experimental results. Recently, Shi et al. studied the PECs of six low-lying electronic states ($X^1\Sigma^+$, $a^3\Pi$, $a'^3\Sigma^+$, $d^3\Delta$, $e^3\Sigma^-$, and $A^1\Pi$) of CS by means of the CASSCF/MRCI method with large correlation-consistent basis sets.[20] Excitation energies, equilibrium bond distances, as well as vibrational and rotational constants of the states were obtained in their calculation; however, perturbations between different states were not addressed.

As we already knew, with the aid of rapid development of high-resolution spectroscopic techniques as well as high-level ab initio calculations, our understanding of the electronic states of the CS molecule is blossoming. New emission bands and more reliable spectroscopic parameters have been continually reported in the literature. However, there is still lacking of a complete picture of perturbations between the states of the CS molecule, which play a significant role in the spectroscopic and dynamic characters of the states. Particularly, SOC is an important state perturbation of the CS molecule. It is expected that the same Ω components of two different Λ−S states can exhibit avoided crossing phenomena due to the SOC effect, and the PECs near avoided crossing regions become more complicated.

In the present work, we carried out an ab initio study on the low-lying electronic states of CS. The PECs of 18 Λ−S states as well as those of 50 Ω states generated from the Λ−S states were calculated. The spectroscopic constants of the bound states were obtained from the calculated PECs. The state perturbations of the $a^3\Pi$ and $A^1\Pi$ states with other low-lying electronic states were discussed in detail, based on the calculated spin−orbit matrix as well as the PECs of the Ω states. Finally, the allowed transition dipole moments as well as the lifetimes of the five lowest vibrational states of the $A^1\Pi_1$, $A'^1\Sigma^+_{0^+}$, and $a^3\Pi_i$ states were obtained.

METHODS AND COMPUTATIONAL DETAILS

In the present study, the ab initio calculations were performed with the Molpro2010[21] suite of quantum chemical package designed by Werner et al. The symmetry point group of the CS molecule is $C_{\infty v}$. However, due to the limit of the MOLPRO program, all of the calculations were carried out in the C_{2v} subgroup of the $C_{\infty v}$ point group. The four different irreducible representations for the C_{2v} point group are A_1, A_2, B_1, and B_2. The correlating relationships between irreducible representations of the $C_{\infty v}$ and C_{2v} point groups are $\Sigma^+ = A_1$, $\Pi = B_1 + B_2$, $\Delta = A_1 + A_2$, and $\Sigma^- = A_2$. In the subsequent calculations, we described the carbon atom with the contracted augmented correlation-consistent polarized quintuple zeta Gaussian-type all-electron aug-cc-pwCV5Z basis set[22,23] [15s,9p,5d,4f,3g,2h] and the sulfur atom with the aug-cc-pwCV5Z basis set[23,24] [21s,13p,5d,4f,3g,2h]. At a series of given internuclear distances between 1.2 and 3.5 Å, the molecular orbitals (MOs) of the ground state were first calculated through the Hartree−Fock (HF) self-consistent field method. To generate balanced MOs used in subsequent correlation calculations, the state-averaged complete active space self-consistent field (SA-CASSCF) calculations[25,26] were carried out for the orbital optimization by using the previous HF MOs as the starting orbitals. A total of 18 Λ−S states, which are two $^1\Sigma^+$, two $^1\Pi$, one $^1\Sigma^-$, one $^1\Delta$, two $^3\Sigma^+$, two $^3\Pi$, one $^3\Sigma^-$, one $^3\Delta$, two $^5\Sigma^+$, two $^5\Pi$, one $^5\Sigma^-$, and one $^5\Delta$, were considered simultaneously in SA-CASSCF calculations. In the CASSCF calculations, active space was composed of eight MOs corresponding to C 2s2p and S 3s3p valence orbitals. The $2s^22p^2$ valence electrons of C and the $3s^23p^4$ valence electrons of S were placed into the active space. Further, by utilizing all configurations in the configuration-interaction (CI) expansion of the CASSCF wave functions as a reference wave function, the energies of 18 Λ−S states were calculated by the internally contracted multireference configuration interaction method with the Davidson correction (MRCI+Q).[27−29] The inner-shell $1s^2$ electrons of the C and S atoms were put into the core orbitals, while the $2s^22p^6$ electrons of the S atom were correlated to account for the core−valence correlations. That is, a total 18 electrons in CS (excluding the 1s orbitals) were correlated in MRCI+Q calculations.

In the above calculations, the scalar relativistic effects were taken into account via the second-order Douglas−Kroll[30] and Hess[31] one-electron integrals. The spin−orbit matrix elements were calculated by utilizing the state interaction method with the full Breit−Pauli Hamiltonian (H_{BP}),[32] so that the spin−orbit eigenstates were determined by diagonalizing $\hat{H}^{el} + \hat{H}^{SO}$ in the basis eigenfunctions of $\hat{H}^{el}$. In the SOC effect calculations, the $\hat{H}^{el}$ matrix elements were acquired from MRCI+Q computations, but the $\hat{H}^{SO}$ matrix elements were acquired from MRCI wave functions. The PECs were mapped by linking the energy points of electronic states considering the avoided crossing rule between the electronic states with the same Ω symmetry.

On the basis of PECs of the bound Λ−S and Ω electronic states, we then solved the nuclear Schrödinger equations using the numerical integration LEVEL procedure designed by Le Roy[33] to obtain the corresponding vibrational energy levels, vibrational wave functions, FCFs, and spectroscopic parameters.

RESULTS AND DISCUSSION

A. PECs of the Low-Lying Λ−S States. The 18 Λ−S states related to the lowest dissociation limit ($C(^3P) + S(^3P)$) of CS were calculated with the MRCI+Q method using aug-cc-pwCV5Z basis set. The PECs for all 18 Λ−S electronic states are shown in Figure 1. For visual clarity, we present the singlet/triplet Λ−S states and the quintet Λ−S states in the panels (a) and (b), respectively, together with the ground state $X^1\Sigma^+$ in each figure. The calculating step lengths of the computed electronic states were 0.05 Å for R = 1.2−2.6 Å and 0.1 Å for R = 2.7−3.5 Å. Table 1 lists the computed spectroscopic constants of CS, including adiabatic transition energies T_e, harmonic vibrational frequencies ω_e, anharmonic terms $\omega_e x_e$, rotational constants B_e, and the equilibrium distance R_e. For comparison, we also list the results of previous experimental and theoretical studies,[15,20,34] where available.

Five singlet states and six triplet states are correlated to the lowest dissociation limit of CS. As shown in Figure 1a, there are no typical repulsive states among these 12 states. For singlet states, the ground state $X^1\Sigma^+$ and the excited states $A^1\Pi$, $1^1\Sigma^-$, and $1^1\Delta$ have deep potential wells in the PECs; the $A'^1\Sigma^+$ state is weekly bounded, and the $2^1\Pi$ state is also weekly bounded at R_e = 1.75 Å but turns out to be repulsive at long R distance.

dx.doi.org/10.1021/jp4002516 | J. Phys. Chem. A 2013, 117, 2373−2382

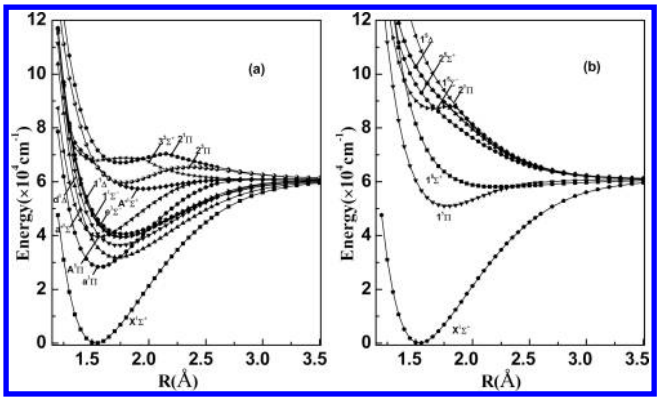

Figure 1. MRCI+Q PECs of the ground and low-lying Λ−S electronic states with singlet and triplet (a) and quintet (b) spin multiplicities, respectively.

Except for the $3^3\Sigma^+$ state, which is weekly bounded at R_e = 1.55 Å but repulsive at long R distance, all triplet states have deep potential wells. The PECs of the singlet and triplet states in Figure 1a agree very well with those reported by Hochlaf et al.[35] Our computed spectroscopic constants of the low-lying bound states are in relatively good agreement with previously available experimental[15,34] and theoretical results,[20,35] as shown in Table 1. For $X^1\Sigma^+$, $a^3\Pi$, $a'^3\Sigma^+$, $d^3\Delta$, $e^3\Sigma^-$, and $A^1\Pi$ states, the differences between our calculation and the experimental results[15,34] are 1143−1290, 7.9−13.4, 0.05−0.9, and 0.0003−0.006 cm^{-1} and 0.0004−0.007 Å for T_e, ω_e, $\omega_e x_e$, B_e, and R_e, respectively. The largest discrepancy is the vibrational constants of the $A'^1\Sigma^+$ state, of which our calculation results are about 100 and 15 cm^{-1} larger than the experimental results[15,34] for ω_e and $\omega_e x_e$, respectively. The $1^1\Sigma^-$, $1^1\Delta$, and $2^3\Pi$ states have not been experimentally observed or theoretically studied in the literature.

No experimental studies about the quintet states of CS have been reported before, and the only theoretical investigation is of the $1^5\Pi$ state by Hochlaf et al.[35] Our results indicate that all of the quintet states have T_e's larger than 50000 cm^{-1}. The lowest quintet state is the bounded $1^5\Pi$ state, of which the vibrational and rotational constants are listed in Table 1, in good agreement with the results of ref 35. Almost all excited quintet states are typically repulsive. Although the $1^5\Sigma^+$ state is weekly bounded at R_e = 2.23 Å, it crosses with other repulsive quintet states and thus may lead to predissociation.

Table 1. Computed and Experimental Spectroscopic Constants of CS[a]

state		T_e (cm^{-1})	ω_e (cm^{-1})	$\omega_e x_e$ ((cm^{-1})	B_e (cm^{-1})	R_e (Å)	configuration at R = 1.55 Å (%)
$X^1\Sigma^+$	this work	0	1298.5	6.6533	0.8204	1.5346	$5\sigma^2 6\sigma^2 7\sigma^2 2\pi^4$(90)
	expt.[b]	0	1285.1	6.46	0.8200	1.5349	
	expt.[c]	0	1285.2	6.502	0.8200	1.535	
	calc.[d]	0	1280.3	6.4824	0.8171	1.538	
$a^3\Pi$	this work	28249	1143.8	7.7702	0.7851	1.5687	$5\sigma^2 6\sigma^2 7\sigma^1 2\pi^4 3\pi^1$(92)
	expt.[d]	27661	1135.1	7.73	0.7851	1.5687	
	expt.[c]	27030	1135.4	7.747	0.7848	1.5691	
	calc.[d]	28233	1133.9	7.6016	0.7831	1.571	
$a'^3\Sigma^+$	this work	31839	839.66	4.9977	0.6522	1.7212	$5\sigma^2 6\sigma^2 7\sigma^2 2\pi^3 3\pi^1$(95)
	expt.[b]	31331	830.7	5.04	0.6489	1.725(5)	
	expt.[c]	30696	829.24	4.943	0.6473	1.728	
	calc.[d]	32004	833.44	5.1984	0.65	1.724	
$d^3\Delta$	this work	36331	805.17	4.8155	0.6379	1.7403	$5\sigma^2 6\sigma^2 7\sigma^2 2\pi^3 3\pi^1$(93)
	expt.[b]	35675	795.6	4.91	0.6367	1.7420	
	expt.[c]	35041	796.17	4.966	0.6369	1.742	
	calc.[d]	35730	795.37	4.6526	0.635	1.744	
$e^3\Sigma^-$	this work	39323	763.51	4.8528	0.6239	1.7598	$5\sigma^2 6\sigma^2 7\sigma^2 2\pi^3 3\pi^1$(93)
	expt.[b]	38683	752	4.(7)	0.619(4)	1.766	
	expt.[c]	38041	752.93	4.955	0.6225	1.762	
	calc.[d]	38737	751.32	4.8265	0.6204	1.764	
$A^1\Pi$	this work	39514	1080.9	10.428	0.7862	1.5677	$5\sigma^2 6\sigma^2 7\sigma^1 2\pi^4 3\pi^1$(87)
	expt.[b]	38904	1073.(4)	10.(1)	0.7800	1.573(9)	
	expt.[c]	38255	1077.23	10.639	0.7876	1.566	
	calc.[d]	38803	1075.08	10.045	0.7847	1.569	
$1^1\Sigma^-$	this work	39554	752.31	5.0810	0.6187	1.7672	$5\sigma^2 6\sigma^2 7\sigma^2 2\pi^3 3\pi^1$(92)
$1^1\Delta$	this work	40384	729.53	4.9994	0.6122	1.7765	$5\sigma^2 6\sigma^2 7\sigma^2 2\pi^3 3\pi^1$(92)
$1^5\Pi$	this work	50939	762.99	11.349	0.6124	1.7764	$5\sigma^2 6\sigma^2 7\sigma^1 2\pi^3 3\pi^2$(94)
	calc.[e]	50167	731.8	11.32	0.5992	1.80	
$A'^1\Sigma^+$	this work	57371	569.84	22.996	0.5137	1.9399	$5\sigma^2 6\sigma^2 7\sigma^1 2\pi^4 8\sigma$(44)
							$5\sigma^2 6\sigma^2 7\sigma^2 2\pi^3 3\pi^1$(31)
	expt.[b]	56505	462.4	7.46	0.511(4)	1.944	
	expt.[c]	55864	462.42	7.458	0.5114	1.944	
$2^3\Pi$	this work	59667	772.53	14.510	0.6130	1.7754	$5\sigma^2 6\sigma^2 7\sigma^1 2\pi^3 3\pi^2$(73)
$1^5\Sigma^+$	this work	58120	268.74	6.257	0.3921	2.2345	$5\sigma^2 6\sigma^2 7\sigma^2 2\pi^3 3\pi^2$(93)

[a]Note: For the experimental values, the inaccuracy of measurement is depicted in the bracket. [b]Reference 34. [c]Reference15. [d]Reference 20. [e]Reference 35.

dx.doi.org/10.1021/jp4002516 | J. Phys. Chem. A 2013, 117, 2373−2382

B. Analysis of the Spin−Orbit Perturbation to $a^3\Pi$ and $A^1\Pi$ States. As indicated in Figure 1 and Table 1, there exists large state density with T_e between 28000 and 40500 cm^{-1}, that is, seven singlet and triplet Λ−S states, $A^1\Pi$, $1^1\Sigma^-$, $1^1\Delta$, $a^3\Pi$, $a'^3\Sigma^+$, $d^3\Delta$, and $e^3\Sigma$, lie in the energy region. This will certainly lead to state perturbation via, for example, SOC. A zooming view of PECs of the states in the energy region is presented in Figure 2, together with the vibrational levels $\nu_A' = 0-2$ of the

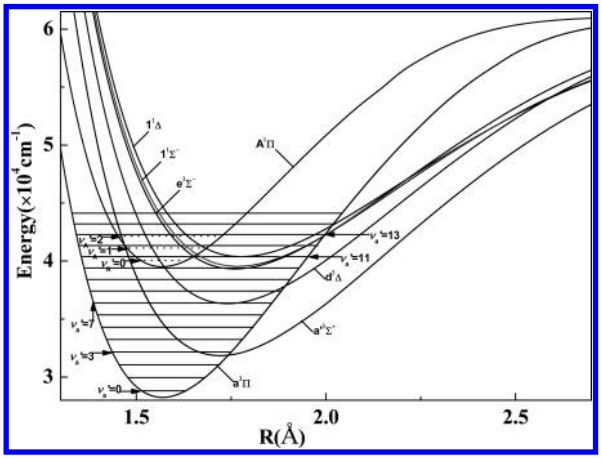

Figure 2. A zooming view of the crossing region of the PECs for electronic states $a^3\Pi$ and $A^1\Pi$ together with the position of vibrational energy levels indicated.

$A^1\Pi$ state and $\nu_a' = 0-15$ of the $a^3\Pi$ state. It can be seen that apparent curve crossings occur between the $a^3\Pi$ state or the $A^1\Pi$ state and the other five states, $a'^3\Sigma^+$, $d^3\Delta$, $e^3\Sigma^-$, $1^1\Delta$, and $1^1\Sigma^-$ at the internuclear distance ranging from 1.4 to 2.1 Å. The state perturbation may not result in dissociation because all seven states are bounded with deep potential wells. However, it could lead to avoided crossing of the states and affect the line intensity, position, and shape of the spectrum, as well as the lifetimes of the states. In the following, we will mainly discuss the SOC effect of the $a^3\Pi$ state and the $A^1\Pi$ state with other electric excited states of CS.

As shown in Figure 2, the $a^3\Pi$ state crosses with the $a'^3\Sigma^+$, $d^3\Delta$, $e^3\Sigma^-$,$1^1\Delta$, and $1^1\Sigma^-$ states at R = 1.75, 1.91, 1.99, 1.99, and 2.02 Å, near $\nu_a' = 3$, 8, 13, 13, and 14, respectively. Because all of the crossing points lie at $\nu_a' > 2$, the vibrational states $\nu_a' = 0$, 1, and 2 of the $a^3\Pi$ state are free from strong interaction with other electronic states. The crossing points between the $A^1\Pi$ state and the triplet states $a'^3\Sigma^+$, $d^3\Delta$, and $e^3\Sigma^-$ are around R = 1.47, 1.57, and 1.65 Å, respectively. In contrast to the $a^3\Pi$ state, the five crossing points are found located in the three lowest vibrational levels, $\nu_A' = 0$, 1, and 2, of the $A^1\Pi$ state. Hence, the perturbations arising from interactions may be important for $\nu_A' = 0$, 1, and 2 levels of the $A^1\Pi$ state. As restricted by the selection rules of SOC of diatomic molecules, there is no SOC effect between the singlet states, $A^1\Pi$ and $1^1\Delta$ ($1^1\Sigma^-$). The crossing points between the $a^3\Pi$ and $A'^1\Sigma^+$ states is located close to the first dissociation limit and will not be discussed in this work.

To further illuminate the perturbation of the states, we calculated spin−orbit matrix elements between two interacting excited states to analyze the SOC effect of the $A^1\Pi$ and $a^3\Pi$ states. Figure 3 shows the absolute values of nonvanishing spin−orbit matrix elements involving the $A^1\Pi$ and $a^3\Pi$ states as a function of the internuclear distance. As the C−S distance

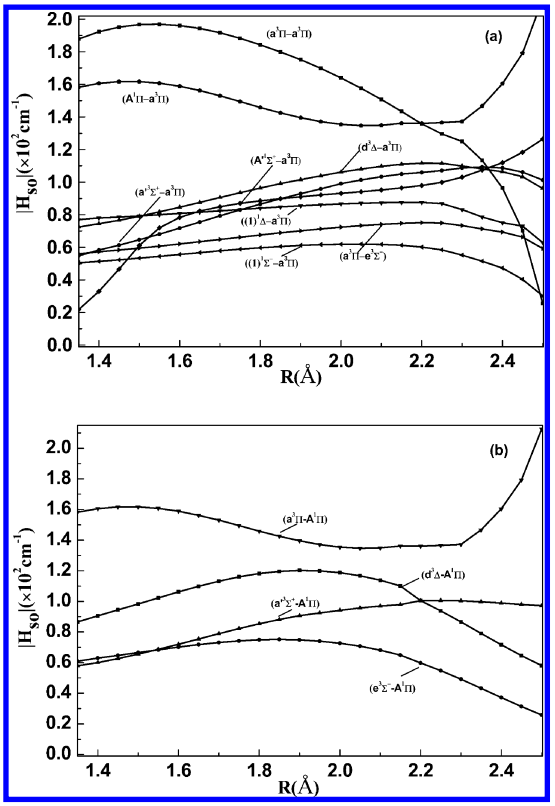

Figure 3. Evolution of the absolute values of spin−orbit matrix elements along the internuclear distance corresponding to the $a^3\Pi$ state (a) and $A^1\Pi$ state (b) in the curve crossing region.

varies, the spin−orbit matrix elements present similar behavior for the coupling between the $a^3\Pi$ state and the $a'^3\Sigma^+$, $d^3\Delta$, $e^3\Sigma^-$, $1^1\Delta$, or $1^1\Sigma^-$ state, but it is different for ($a^3\Pi-a^3\Pi$), ($a^3\Pi-A'^1\Sigma^+$), and ($A^1\Pi-a^3\Pi$) (Figure 3a). This is probably related to the same electronic configuration of the $a'^3\Sigma^+$, $d^3\Delta$, $e^3\Sigma^-$, $1^1\Delta$, and $1^1\Sigma^-$ states, which is mainly described by $5\sigma^2 6\sigma^2 7\sigma^2 2\pi^3 3\pi^1$ at both R = 1.55 Å and a long internuclear distance (R = 2.1 Å). Moreover, the $A^1\Pi$ state and the $a^3\Pi$ state also have the same configuration, mainly $5\sigma^2 6\sigma^2 7\sigma^1 2\pi^4 3\pi^1$ at R = 1.55 Å and $5\sigma^2 6\sigma^2 7\sigma^1 2\pi^4 3\pi^1$ and $5\sigma^2 6\sigma^2 7\sigma^1 2\pi^3 3\pi^2$ at R = 2.1 Å. As shown in Figure 3b, the spin−orbit matrix elements involving the $A^1\Pi$ state have similar dependence on the C−S distance as those involving the $a^3\Pi$ state, despite the fact that the maximum of the elements are at different R values.

At the crossing points, the values of spin−orbit integrals of $a^3\Pi-a'^3\Sigma^+$, $a^3\Pi-d^3\Delta$, $a^3\Pi-e^3\Sigma^-$, $a^3\Pi-1^1\Delta$, and $a^3\Pi-1^1\Sigma^-$ are 82.9, 102.2, 72.3, 87.0, and 61.8 cm^{-1}, respectively, while those of $A^1\Pi-a'^3\Sigma^+$, $A^1\Pi-d^3\Delta$, and $A^1\Pi-e^3\Sigma^-$ are 63.6, 104.0, and 71.7 cm^{-1}, respectively. Previous electronic spin−orbit interaction parameters[36] deduced from the UV spectrum for $a^3\Pi-a'^3\Sigma^+$ at R = 1.74, $a^3\Pi-d^3\Delta$ at R = 1.90, and $a^3\Pi-e^3\Sigma^-$ at R = 1.99 are 78.5, 103.6, and 74.3 cm^{-1}, respectively, which were in good agreement with our present theoretical values. The previously reported spin−orbit interaction parameters[36] between the $A^1\Pi$ sate and $a'^3\Sigma^+$, $d^3\Delta$, and $e^3\Sigma^-$ are 60.8, 102.3, and 73.2 cm^{-1}, respectively. Our computed values agree with the experimental values.[36]

C. PECs of the Low-Lying Ω States. When the SOC effect is taken into account, different Λ−S states with common Ω will recombine. We used Λ−S MRCI wave functions as the basis to solve the eigenequation of the full Breit−Pauli Hamiltonian and

dx.doi.org/10.1021/jp4002516 | J. Phys. Chem. A 2013, 117, 2373−2382

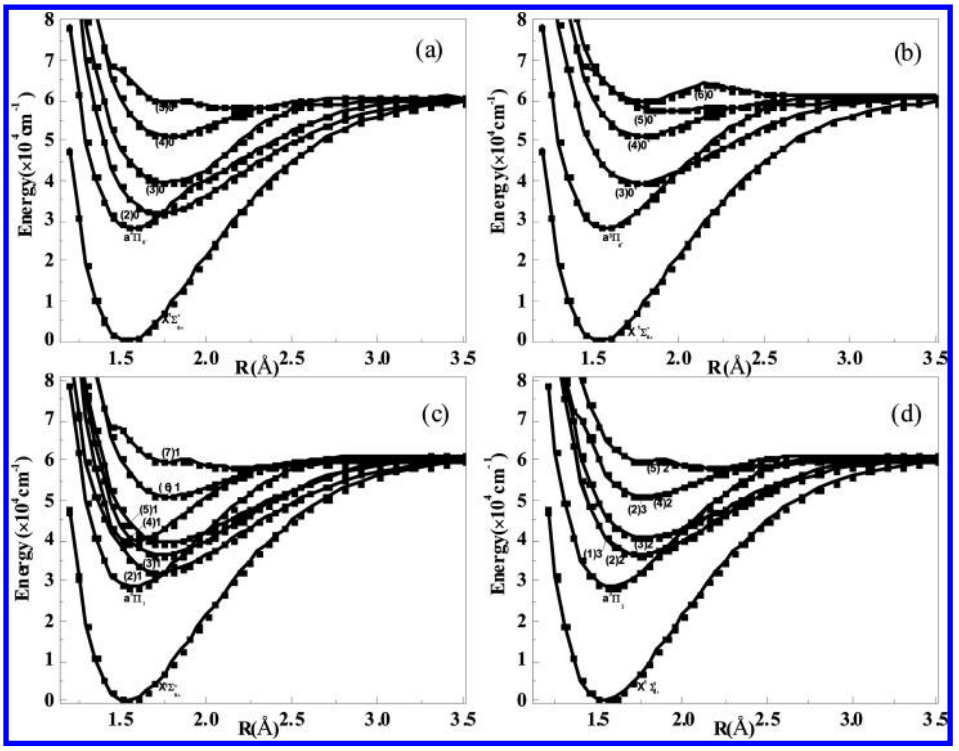

Figure 4. PECs with the SOC effect of the low-lying electronic state of the CS molecule for Ω = (a) 0^-, (b) 0^+, (c) 1, and (d) 2 and 3 states.

plotted the PECs by connecting the computed eigenvalues of the corresponding electronic state. There are a total of 50 Ω states generated from the 18 Λ−S states, which correlate with the lowest dissociation $S(^3P) + C(^3P)$ of the CS molecule. PECs for all 50 Ω states have been calculated; however, we will not discuss the repulsive high-lying states in this study. There are 25 low-lying bound Ω states, which are mainly concentrated in the excitation energy range of 28000−63000 cm^{-1}. Their PECs are shown in Figure 4, including five $\Omega = 0^-$ states, six $\Omega = 0^+$ states, seven Ω = 1 states, five Ω = 2 states, and two Ω = 3 states. The dissociation limits for the Ω states and the corresponding energy splitting are listed in Table 2. The computed energy splitting is 13 cm^{-1} for $^3P_1-^3P_0$ of C, 39 cm^{-1} for $^3P_2-^3P_0$ of C, 400 cm^{-1} for $^3P_1-^3P_2$ of S, and 599 cm^{-1} for $^3P_0-^3P_2$ of S, which are consistent with the experimental values.[37]

Table 2. Dissociation Relationship of the Low-Lying Ω States of CS

atomic state (C + S)	Ω state	energy (cm^{-1}) expt.[37]	energy (cm^{-1}) this work
$^3P_0 + ^3P_2$	$2,1,0^+$	0	0
$^3P_1 + ^3P_2$	$3,2,2,1,1,1,0^+,0^-,0^-$	16	13
$^3P_2 + ^3P_2$	$4,3,3,2,2,2,1,1,1,1,0^+,0^+,0^+,0^-,0^-$	43	39
$^3P_0 + ^3P_1$	$1,0^-$	396	400
$^3P_1 + ^3P_1$	$2,1,1,0^+,0^+,0^-$	412	413
$^3P_2 + ^3P_1$	$3,2,2,1,1,1,0^+,0^-,0^-$	439	439
$^3P_0 + ^3P_0$	0^+	574	599
$^3P_1 + ^3P_0$	$1,0^-$	590	612
$^3P_2 + ^3P_0$	$2,1,0^+$	617	638

On the basis of the computed Ω-state PECs, the spectroscopic constants of the CS molecule are numerically obtained, which are listed in Table 3. The ground state $X0^+$ is composed of 100% $X^1\Sigma^+$ Λ−S state; hence, the spectroscopic parameters of $X0^+$ given in Table 3 is the same as those of the Λ−S ground state $X^1\Sigma^+$. Under the SOC effect, a Λ−S state will split into different Ω states. The states with the same Ω could lead to strong SOC, thus the avoided crossing in the PECs. As a result, the computed spectroscopic constants for the

Table 3. Computed Spectroscopic Constants of Low-Lying Ω States in CS

state	T_e (cm^{-1})	ω_e (cm^{-1})	$\omega_e x_e$ (cm^{-1})	B_e (cm^{-1})	R_e (Å)
$X0^+$	0.0	1298.5	6.6536	0.8204	1.5346
$(a^3\Pi)0^-$	28149	1093.4	21.798	0.7853	1.5688
$(a^3\Pi)0^+$	28150	1094.1	21.851	0.7853	1.5688
$(a^3\Pi)1$	28247	1088.6	21.858	0.7853	1.5688
$(a^3\Pi)2$	28347	1206.5	16.352	0.7851	1.5686
(2)1	31837	1246.1	24.609	0.6623	1.7163
$(2)0^-$	31862	1247.1	23.756	0.6638	1.7132
(3)1	36198	852.41	6.3065	0.6367	1.7413
(1)3	36279	892.18	4.0101	0.6370	1.7401
(2)2	36424	902.71	4.6974	0.6375	1.7401
(4)1	39335	583.67	−11.369	0.6006	1.7530
$(3)0^+$	39325	753.84	−3.1403	0.6239	1.7598
$(3)0^-$	39558	746.55	−3.7396	0.6187	1.7672
(5)1	40479	1527.5	40.343	0.7102	1.6522
(3)2	40592	715.52	−3.8602	0.6118	1.7771
(2)3	50762	762.9	11.125	0.6121	1.7768
(4)2	50850	758.49	10.813	0.6122	1.7766
(6)1	50939	761.49	11.159	0.6124	1.7764
$(4)0^+$	51028	755.61	10.484	0.6125	1.7763
$(4)0^-$	51030	758	10.671	0.6125	1.7762
$(5)\ 0^+$	57373	437.47	12.607	0.5196	1.9399
$(5)0^-$	58128	393.24	12.471	0.3977	2.2283
(7)1	58147	382.47	11.239	0.3990	2.1871
(5)2	58147	469.47	16.268	0.3996	2.1818
$A'0^+$	59748	730.69	8.9333	0.6139	1.7768

dx.doi.org/10.1021/jp4002516 | J. Phys. Chem. A 2013, 117, 2373−2382

Table 4. Composition of Ω States of CS at Different Bond Distances

state	r (Å)	$^1\Sigma^-$	$^1\Sigma^+$	$^1\Pi$	$^1\Delta$	$^3\Sigma^-$	$^3\Sigma^+$	$^3\Pi$	$^3\Delta$	state	r (Å)	$^1\Sigma^-$	$^1\Sigma^+$	$^1\Pi$	$^1\Delta$	$^3\Sigma^-$	$^3\Sigma^+$	$^3\Pi$	$^3\Delta$
$X0^+$	1.55		100							(2)2	1.55								99.8
	1.6		100								1.6								99.8
	1.65		100								1.65								99.8
	1.7		100								1.7								99.8
	1.75		100								1.75								99.7
	1.8		100								1.8								99.6
	2.0		100								2.0							99.2	0.6
$(a^3\Pi)0^-$	1.55							99.9		(4)1	1.55								99.3
	1.6							99.9			1.6			99.01					
	1.65							99.9			1.65			68.39		31.52			
	1.7						0.6	99.4			1.7					99.74			
	1.75						76.4	23.6			1.75					99.86			
	1.8						99.4	0.6			1.8					99.86			
	2.0						99.9				2.0					22.62		77.07	
$(a^3\Pi)0^+$	1.55							100		$(3)0^+$	1.55					100			
	1.6							100			1.6					100			
	1.65							100			1.65					100			
	1.7							100			1.7					100			
	1.75							100			1.75					100			
	1.8							100			1.8					100			
	2.0					53.7		46.3			2.0					46.3		53.7	
$(a^3\Pi)1$	1.55							100		(5)1	1.55					99.9			
	1.6							100			1.6					99.9			
	1.65							99.9			1.65			31.48		68.4			
	1.7						0.3	99.7			1.7			99.77					
	1.75						91.6	8.4			1.75			99.91					
	1.8						99.6	0.3			1.8			99.94					
	2.0						99.9				2.0			99.96					
$(a^3\Pi)2$	1.55							100		$(3)0^-$	1.55	99.8							
	1.6							100			1.6	99.8							
	1.65							100			1.65	100							
	1.7							100			1.7	99.8							
	1.75							99.9			1.75	100							
	1.8							99.8	0.15		1.8	100							
	2.0							0.2	99.8		2.0	56.6						43.4	
(2)1	1.45			99.6			0.4			(3)2	1.55				99.8				
	1.55						99.9				1.6				99.8				
	1.6						99.9				1.65				99.8				
	1.65						99.9				1.7				100				
	1.7						99.6				1.75				99.7				
	1.75						8.4	91.6			1.8				99.7				
	1.8							99.6			2.0				96.7				0.6
	2.0								99.8	(5) 0^+	1.55							99.9	

dx.doi.org/10.1021/jp4002516 | J. Phys. Chem. A 2013, 117, 2373−2382

Table 4. continued

state	r (Å)	$^1\Sigma^-$	$^1\Sigma^+$	$^1\Pi$	$^1\Delta$	$^3\Sigma^-$	$^3\Sigma^+$	$^3\Pi$	$^3\Delta$	state	r (Å)	$^1\Sigma^-$	$^1\Sigma^+$	$^1\Pi$	$^1\Delta$	$^3\Sigma^-$	$^3\Sigma^+$	$^3\Pi$	$^3\Delta$
(2)0^-	1.55						100				1.6							99.9	
	1.6						100				1.65							99.9	
	1.65						99.9				1.7		99					1	
	1.7						99.4	0.6			1.75		99.9						
	1.75						23.6	76.4			1.8		99.9						
	1.8							99.9			1.9		99.9						
	1.9							99.9			2.0		99.9						
	2.0	43.3						56.6		(6) 0^+	1.55		100						
(3)1	1.55			99.2							1.6		100						
	1.6								100		1.65		100						
	1.65								100		1.7		1					99	
	1.7								100		1.75							99.9	
	1.75								100		1.8							99.9	
	1.8								100		1.9							99.9	
	1.90							68.57	31.32		2.0							99.9	
	1.95							98.74	0.72										
	2.0					77.24		22.64											
(1)3	1.55								100										
	1.6								100										
	1.65								100										
	1.7								100										
	1.75								100										
	1.8								100										
	2.0								100										

dx.doi.org/10.1021/jp4002516 | J. Phys. Chem. A 2013, 117, 2373−2382

Ω states in Table 5 would be quite different from those for the pure Λ−S states in Table 1.

We now further discuss the SOC effects as well as the resulting avoided crossing phenomena of CS based on the PECs of the Ω states in Figure 4 as well as the composition of the Ω states at different C−S bond distances. The latter is presented in Table 4. We still focus on the coupling involving the $a^3\Pi$ state and the $A^1\Pi$ state. As stated in the previous section, the $a^3\Pi$ state crosses with the compacted spaced $a'^3\Sigma^+$, $d^3\Delta$, $e^3\Sigma^-$, $1^1\Delta$, and $1^1\Sigma^-$ states in the internuclear distances region of 1.7−2.0 Å (Figure 2), and there is a nonvanishing spin−orbit matrix between each coupled states (Figure 3). Restricted by the selection rules, only the states with the same Ω symmetries can interact via SOC. Thus, SOC effects involving the $a^3\Pi$ state result in eight avoided crossings in the PECs (Figure 4). The Λ−S state compositions for the Ω states change sharply around the internuclear distance where the crossing occurs, which strongly indicates the coupling between the states (Table 4). For instance, the SOC between the $\Omega = 0^-$ or 1 components of the $a^3\Pi$ state and the $a'^3\Sigma^+$ state produces two avoided crossings at $R \approx 1.75$ Å (see Figure 4a and c). As a result, the dominant composition of $(a^3\Pi)0^-$ changes from 99.4% $^3\Pi$ at $R = 1.7$ Å to 99.4% $^3\Sigma^+$ at $R = 1.8$ Å, and the dominant composition of $(a^3\Pi)1$ changes from 99.7% $^3\Pi$ at $R = 1.7$ Å to 99.6% $^3\Sigma^+$ at $R = 1.8$ Å (Table 4).

For the $A^1\Pi$ state, there is only one component of $\Omega = 1$; therefore, three avoided crossings occur between the $A^1\Pi$ state and the $a'^3\Sigma^+$, $d^3\Delta$, and $e^3\Sigma^-$ states with $\Omega = 1$. As shown in Figure 4c, the PECs of (2)1 and (3)1 states have one avoided crossing point at $R = 1.45$ Å, and those of (3)1−(4)1 and (4)1−(5)1 pairs have two avoided crossing points at $R = 1.55$ and $R = 1.65$ Å, respectively. Table 4 shows that the dominant Λ−S state composition of the (2)1 state changes from $^1\Pi$(99.6%) at $R = 1.45$ Å to $^3\Sigma^+$(99.9%) at $R = 1.55$ Å, that of (3)1 state changes from 99.2% $^1\Pi$ at $R = 1.55$ Å to 100% $^3\Delta$ at $R = 1.60$ Å, and that of (4)1 state changes from 99.3% $^3\Delta$ at $R = 1.55$ Å to 99.74% $^3\Sigma^-$ at $R = 1.70$ Å. The wave function of the (4)1 state at $R = 1.65$ Å is a mixture of $^1\Pi$ (68.4%) and $^3\Sigma^-$ (31.5%), which implies that the transition properties of nearby vibrational levels of the $A^1\Pi$ state will be heavily polluted by the $e^3\Sigma^-$ state. Due to avoided crossing between $A^1\Pi$ and $a'^3\Sigma^+$, $d^3\Delta$, or $e^3\Sigma^-$, the PEC shapes of the $\Omega = 1$ state (corresponding to Λ−S $A^1\Pi$) have obvious variation.

Recently, Li et al.[16] performed perturbation analysis of the $\nu = 6$ vibrational level of the $d^3\Delta$ state based on its near-infrared absorption spectrum. Their experimental results indicate that due to the spin−orbit interaction, a large percentage of $d^3\Delta_1$ character is shared by $a^3\Pi$ and $A^1\Pi$ states. This was confirmed by the present theoretical results. As listed in Table 4, the PEC of 3(1) in the range of its Franck−Condon region ($R = 1.6$−1.8) is composed with $d^3\Delta_1$, whereas that of 3(1) exhibits obvious $A^1\Pi_1$ character at $R = 1.55$ Å. The wave function of 3(1) at $R = 1.90$ is a mixture of $d^3\Delta$ (31.3%) and $a^3\Pi$ (68.6%), and that of 3(1) at 1.95 Å is dominant (98.7%) by $a^3\Pi$ state. Our computations found that the classical turning points of the $\nu = 6$ level of the 3(1) state are located at $R = 1.50$ and 1.95 Å, respectively.

D. Electronic Transition Dipole Moments and Radiative Lifetimes. Figure 5 shows the electronic transition dipole moments (TDMs) of CS from the ground state to the bound Ω excited states as functions of the internuclear distance. Two sets of TDMs, the $(5-6)0^+-(X^1\Sigma^+)0^+$ and $(2-5)1-(X^1\Sigma^+)0^+$ transitions, are plotted in the figure, which correspond to the

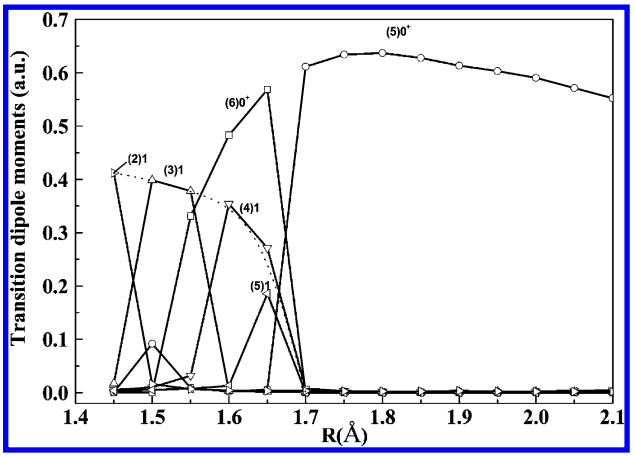

Figure 5. Evolution of the allowed transition dipole moment for CS from bound excited Ω states to the ground state along the internuclear distance. (The dotted line is used to guide the eyes.)

strongest allowed singlet−singlet transitions, $A^1\Pi-X^1\Sigma^+$ (Ω 1−0^+) and $A'^1\Sigma^+-X^1\Sigma^+$ (Ω 0^+-0^+). The TDMs for triplet−singlet forbidden transitions (such as $a^3\Pi-X^1\Sigma^+$ or $a'^3\Sigma^+-X^1\Sigma^+$) are at least 2 orders of magnitude smaller than those in Figure 5 and are not presented here. For $(5-6)0^+-(X^1\Sigma^+)0^+$ transitions, the TDM values of the $(6)0^+-(X^1\Sigma^+)0^+$ transition are larger at bond lengths between 1.55 and 1.65 Å, while those of the $(5)0^+-(X^1\Sigma^+)0^+$ transition are dominant at bond lengths larger than 1.7 Å. As shown in Table 4, the $A'^1\Sigma^+$ state is the dominant composition of the $(6)0^+$ state at $R < 1.65$ Å and is the dominant composition of the $(5)0^+$ state at $R > 1.65$ Å. The turning point of TDMs at around 1.65 Å could be attributed to the avoided crossing between $(5)0^+$ and $(6)0^+$. The case for TDMs of $(2-5)1-(X^1\Sigma^+)0^+$ transitions is more complicated due to numbers of avoided crossing points found in the region of 1.4−1.7 Å, as shown in Figure 4 and discussed in the above section. By analyzing the compositions of the (2−5)1 Ω states, it is found that the profile (dotted line in Figure 5) of TDMs of $(2-5)1-X^1\Sigma^+_{0^+}$ transitions corresponds to the TDM of the Λ−S transition $A^1\Pi-X^1\Sigma^+$.

Table 5 lists the radiative lifetimes of the five lowest vibrational levels of the $A^1\Pi$, $A'^1\Sigma^+$, and $a^3\Pi$ states, which were computed using our calculated TDMs, the PECs, and vibrational wave functions. The computed radiative lifetimes of the $A^1\Pi$ state are on the order of 100 ns, and those of the $A'^1\Sigma^+$ state are on the order of 10 ns, whereas, that of $a^3\Pi-X^1\Sigma^+$ is on the order of 1 ms. The present computed radiative lifetimes are in relatively good agreement with previous available theoretical and experimental results,[7−11,13,19] as shown in Table 5. It is observed that our computed lifetimes of the $\nu_A' = 0$, 1, and 2 vibrational levels of the $A^1\Pi$ state are generally shorter than the experimental values. As discussed in the previous sections, the crossing points between the $A^1\Pi$ state and the triplet states are located in the $\nu_A' = 0$, 1, and 2 levels of the $A^1\Pi$ state, thus non-Born−Oppenheimer state coupling occurs, leading to deviations of the calculated and experimental values of the lifetimes of these vibrational states.

CONCLUSIONS

The PECs of the low-lying electronic states for the CS molecule were theoretically investigated by the MRCI+Q method with the all-electronic aug-cc-pwCV5Z basis set. The Ω-state PECs including the SOC effect were obtained by diagonalizing the

dx.doi.org/10.1021/jp4002516 | J. Phys. Chem. A 2013, 117, 2373−2382

Table 5. Radiative Lifetimes (in ns) of the Low-Lying Vibrational Levels of $A^1\Pi_1$, $A'^1\Sigma_0^+$, and $a^3\Pi_i$

		radiative lifetimes					
state		$\nu' = 0$	$\nu' = 1$	$\nu' = 2$	$\nu' = 3$	$\nu' = 4$	$\nu' = 5$
$A^1\Pi_1$	this work	159	187	212	251	258	253
	expt.[a]	185(10)	225(20)	220(20)	230(20)	235(20)	225(20)
	expt.[b]	255(25)	339(35)	292(30)	292(30)	292(30)	
	expt.[c]	171(10)					
	expt.[d]	191	199	205	214	222	230
	calc.[e]	167					
$A'^1\Sigma_0^+$	this work	9.19	10	10.36	10.89	11.39	12.13
	expt.[f]						15(2)
$a^3\Pi_0^-$	this work	very long					
$a^3\Pi_0^+$	this work	3.89×10^6	4.08×10^6	4.65×10^6	5.59×10^6	7.2×10^6	8.66×10^6
	expt.[g]	2.3×10^6					
	calc.[g]	3.4×10^6					
$a^3\Pi_1$	this work	1.58×10^6	1.63×10^6	1.71×10^6	1.87×10^6	2.27×10^6	2.4×10^6
	expt.[g]	5.9×10^6					
	calc.[g]	6.4×10^6					
$a^3\Pi_2$	this work	1.06×10^{15}					
	expt.[g]	$>10^9$					
	calc.[g]	very long					

[a]Reference 9. [b]Reference 7. [c]Reference 8. [d]Reference 10. [e]Reference 19. [f]Reference 11. [g]Reference 13.

Hamiltonian containing the SO Breit–Pauli operator in the basis of the Λ–S MRCI wave functions. The scalar relativity correction was taken into account by utilizing the second-order one-electron Douglas–Kroll–Hess method.

The PECs of 18 Λ–S states as well as 50 Ω states generated from Λ–S states were calculated, from which the spectroscopic parameters were obtained, in good agreement with previous available experimental and theoretical results. It was observed that the $a^3\Pi$ and $A^1\Pi$ states cross with $a'^3\Sigma^+$, $d^3\Delta$, $e^3\Sigma^-$, $1^1\Sigma^-$, and $1^1\Delta$ at a bond length region between 1.45 and 2.1 Å. The values of the spin–orbit matrix were calculated in the region of 60–104 cm^{-1} at the crossing points. With the aid of a calculated spin–orbit matrix as well as the PECs of Ω states, we discussed in detail the interactions of the low-lying states, revealing the avoided crossing in the PECs of the states. The allowed transition moments of the Ω states to the ground state were studied, and the lifetimes of five lowest vibrational levels of the $A^1\Pi_1$, $A'^1\Sigma^+_{0^+}$, $a^3\Pi_{0^+}$, $a^3\Pi_1$, and $a^3\Pi_2$ states were evaluated. Our study indicates that the SOC plays an important role in the low-lying excited states for the CS molecule. The present theoretical study will add some understanding and shed more light on the structure and spectroscopic properties of the low-lying electronic states of the CS molecule.

■ ASSOCIATED CONTENT

Supporting Information

Data of PECs of the Λ–S electronic states in Figure 1 are summarized in Table S1. The absolute values of spin–orbit matrix elements along the internuclear distance corresponding to the $a^3\Pi$ state (Figure 3a) and $A^1\Pi$ state (Figure 3b) are summarized in Tables S2 and S3, respectively. Data of PECs of the low-lying Ω states in Figure 4 are summarized in Table S4. Data of the allowed transition dipole moment for CS in Figure 5 are summarized in Table S5. The complete author list of ref 21 is also provided. This material is available free of charge via the Internet at http://pubs.acs.org.

■ AUTHOR INFORMATION

Corresponding Author

*Tel: 86-431-85168817. Fax: 86-431-85168816. E-mail: xuhf@jlu.edu.cn (H.X.); yanbing@jlu.edu.cn (B.Y.).

Notes

The authors declare no competing financial interest.

■ ACKNOWLEDGMENTS

This work was supported by the National Basic Research Program of China (973 Program) (2013CB922200), the National Magnetic Confinement Fusion Science Program of China (2010GB104003), and the National Natural Science Foundation of China (11034003, 11074095, and 11274140). R.L. also acknowledges the financial support by the Natural Science Foundation of Heilongjiang Province (QC2011C092). We acknowledge the High Performance Computing Center (HPCC) of Jilin University for supercomputer time.

■ REFERENCES

(1) Krishna Swamy, K. S.; Tarafdar, S. P. Study of the *A*–*X*(0,0) Band Profile of CS in Comets. *Astron. Astrophys.* **1993**, *271*, 326–334.

(2) Walker, C. K.; Lada, C. J.; Young, E. T.; Maloney, P. R.; Wilking, B. A. Spectroscopic Evidence for Infall Around an Extraordinary IRAS Source in Ophiuchus. *Astrophys. J.* **1986**, *309*, 47–51.

(3) Destree, J. D.; Snow, T. P.; Black, J. H. An Ultraviolet Search for Interstellar CS. *Astrophys. J.* **2009**, *693*, 804–811.

(4) Williams, J. P.; Blitz, L. A. Multitransition CO and CS (2–1) Comparison of a Star-Forming and a Non-Star-Forming Giant Molecular Cloud. *Astrophys. J.* **1998**, *494*, 657–673.

(5) Martín, S.; Martín-Pintado, J.; Mauersberger, R.; Henkel, C.; García-Burillo, S. Sulfur Chemistry and Isotopic Ratios in the Starburst Galaxy NGC 253. *Astrophys. J.* **2005**, *620*, 210–216.

(6) Crawford, F. H.; Shurcliff, W. A. The Band Spectrum of CS. *Phys. Rev.* **1934**, *45*, 860–870.

(7) Smith, W. H. Absolute Transition Probabilities for Some Electronic States of CS, SO and S_2. *J. Quant. Spectrosc. Radiat. Transfer* **1969**, *9*, 1191–1199.

(8) Hynes, A. J.; Brophy, J. H. Laser-Induced Fluorescence Study of Radiative Lifetimes and Quenching Rates in CS $A^1\Pi(\nu = 0)$. *Chem. Phys. Lett.* **1979**, *63*, 93–96.

(9) Carlson, T. A.; Copley, J.; Durić, N.; Erman, P.; Larsson, M. Time Resolved Studies of Collisional Transfer and Radiative Decay of the CS $A^1\Pi$ State. *Chem. Phys.* **1979**, *42*, 81−87.
(10) Mahon, C. A.; Stampanoni, A.; Luque, J.; Crosley, D. R. Transition Probabilities in the $A^1\Pi-X^1\Sigma^+$ System of CS. *J. Mol. Spectrosc.* **1997**, *183*, 18−24.
(11) Dornhoefer, G.; Hack, W.; Langel, W. Electronic Excitation and Quenching of Thiocarbonyl (CS) Formed in the Argon Fluoride Laser Photolysis of Carbon Disulfide. *J. Phys. Chem.* **1984**, *88*, 3060−3069.
(12) Cossart, D.; Horani, M.; Rostas, J. Rotational Analysis of the $a^3\Pi_r-X^1\Sigma^+$ Transition of CS. *J. Mol. Spectrosc.* **1977**, *67*, 283−303.
(13) Fournier, J.; Deson, J.; Vermeil, C.; Robbe, J. M.; Schamps, J. Nonexponential Decay of CS $a^3\Pi-X^1\Sigma^+$ Luminescence. *J. Chem. Phys.* **1979**, *70*, 5703−5707.
(14) Cossart, D. Rotational Analysis of the $d^3\Delta_i-a^3\Pi_r$ Transition of Carbon Monosulfide. *J. Phys. (Paris)* **1980**, *41*, 489−502.
(15) Bergeman, T.; Cossart, D. The Lower Excited States of CS: A Study of Extensive Spin−Orbit Perturbations. *J. Mol. Spectrosc.* **1981**, *87*, 119−195.
(16) Li, C.; Deng, L.; Zhang, Y.; Wu, L.; Yang, X.; Chen, Y. Perturbation Analysis of the $\nu = 6$ Level in the $d^3\Delta$ State of CS Based on Its Near-Infrared Absorption Spectrum. *J. Phys. Chem. A* **2011**, *115*, 2978−2984.
(17) Robbe, J. M.; Schamps, J. Calculations of Perturbation Parameters Between Valence States of CS. *J. Chem. Phys.* **1976**, *65*, 5420−5426.
(18) Wilson, S. Diagrammatic Perturbation Theory. The Ground State of the Carbon Monosulfide Molecule. *J. Chem. Phys.* **1977**, *67*, 4491−4497.
(19) Ornellas, F. R. Transition Moment Function, Transition Probabilities, and Radiative Lifetimes in the $A^1\Pi-X^1\Sigma^+$ System of the CS Molecule. *Chem. Phys. Lett.* **1998**, *296*, 25−33.
(20) Shi, D. H.; Li, W. T.; Zhang, X. N.; Sun, J. F.; Liu, Y. F.; Zhu, Z. L.; Wang, J. M. Effects on Spectroscopic Properties for Several Low-Lying Electronic States of CS Molecule by Core−Valence Correlation and Relativistic Corrections. *J. Mol. Spectrosc.* **2011**, *266*, 27−36.
(21) Werner, H.-J.; Knowles, P. J.; Lindh, R.; Manby, F. R.; Schütz, M.; Celani, P.; Korona, T.; Mitrushenkov, A.; Rauhut, G.; Adler, T. B.; et al. *MOLPRO*, a package of ab initio programs; 2010.
(22) Kendall, R. A.; Dunning, T. H.; Harrison, R. J. Electron Affinities of the First-Row Atoms Revisited. Systematic Basis Sets and Wave Functions. *J. Chem. Phys.* **1992**, *96*, 6796−6806.
(23) Peterson, K. A.; Dunning, T. H. Accurate Correlation Consistent Basis Sets for Molecular Core−Valence Correlation Effects: The Second Row Atoms Al−Ar, and the First Row Atoms B−Ne Revisited. *J. Chem. Phys.* **2002**, *117*, 10548−10560.
(24) Woon, D. E.; Dunning, T. H. Gaussian Basis Sets for Use in Correlated Molecular Calculations. III. The Atoms Aluminum Through Argon. *J. Chem. Phys.* **1993**, *98*, 1358−1371.
(25) Werner, H.; Knowles, P. J. A Second Order Multiconfiguration SCF Procedure with Optimum Convergence. *J. Chem. Phys.* **1985**, *82*, 5053−5063.
(26) Knowles, P. J.; Werner, H.-J. An Efficient Second-Order MCSCF Method for Long Configuration Expansions. *Chem. Phys. Lett.* **1985**, *115*, 259−267.
(27) Werner, H.-J.; Knowles, P. J. An Efficient Internally Contracted Multiconfiguration−Reference Configuration Interaction Method. *J. Chem. Phys.* **1988**, *89*, 5803−5814.
(28) Knowles, P. J.; Werner, H.-J. An Efficient Method for the Evaluation of Coupling Coefficients in Configuration Interaction Calculations. *Chem. Phys. Lett.* **1988**, *145*, 514−522.
(29) Langhoff, S. R.; Davidson, E. R. Configuration Interaction Calculations on the Nitrogen Molecule. *Int. J. Quantum Chem.* **1974**, *8*, 61−72.
(30) Douglas, M.; Kroll, N. M. Quantum Electrodynamical Corrections to the Fine Structure of Helium. *Ann. Phys.* **1974**, *82*, 89−155.
(31) Hess, B. A. Relativistic Electronic-Structure Calculations Employing a Two-Component No-Pair Formalism with External-Field Projection Operators. *Phys. Rev. A* **1986**, *33*, 3742−3748.
(32) Berning, A.; Schweizer, M.; Werner, H.-J.; Knowles, P. J.; Palmieri, P. Spin−Orbit Matrix Elements for Internally Contracted Multireference Configuration Interaction Wavefunctions. *Mol. Phys.* **2000**, *98*, 1823−1833.
(33) Le Roy, R. J. *LEVEL7.7: A Computer Program for Solving the Radial Schrödinger Equation for Bound and Quasibound Levels*; Chemical Physics Research Report CP-661; University of Waterloo: Ontario, Canada, 2005.
(34) Huber, K. P.; Herzberg, G. *Molecular Spectra and Molecular Structure IV, Constants of Diatomic Molecules*; Van Nostrand Reinhold: New York, 1979.
(35) Hochlaf, M.; Chambaud, G.; Rosmus, P.; Andersen, T.; Werner, H. J. Quartet and Sextet States of CS^-. *J. Chem. Phys.* **1999**, *110*, 11835−11840.
(36) Cossart, D.; Bergeman, T. Offdiagonal Spin−Orbit and Apparent Spin−Spin Parameters in Carbon Monosulfide. *J. Chem. Phys.* **1976**, *65*, 5462−5468.
(37) Moore, C. E. *Atomic Energy Levels*; National Bureau of Standard: Washington, DC, 1971.